Influence of Processing Parameters on the Recrystallized Microstructure of Extra-Low-Carbon Steels

C. CAPDEVILA, J.P. FERRER, F.G. CABALLERO, and C. GARCÍA DE ANDRÉS

This article deals with the influence of processing parameters of a new procedure for ferritic rolling on the recrystallized microstructure of extra-low-carbon (ELC) steels. Parameters such as coil transfer temperature and degree of reduction during ferritic rolling are shown to control the morphology of cementite particles and the precipitation of AlN process. The recrystallized grain morphology and the percentage of recrystallization after annealing cycles simulating the industrial coiling process are shown to be strongly influenced by processing parameters.

I. INTRODUCTION

THIN gage hot-rolled strips (<1.2 mm) are nowadays more and more accepted as a low-cost substitute for conventional cold-rolled and annealed sheets. Because of the high-temperature drop in the finishing mill when rolling thin gage strip and the lower deformation resistance of ferrite, warm rolling below the γ-α transformation could be a suitable processing method for thinner gages of low-carbon steels, as has been the object of numerous studies.[1–5] In past years, steelmakers have followed this technology with increasing interest because of the associated decrease in production cost and simultaneous increase in the range of products offered.[2,5]

Focusing on the production of fully recrystallized thin hot strips of extra-low-carbon (ELC) steel for direct application, as-coiled material is fully recrystallized if the finishing rolling temperature (FRT) is low enough (FRT ranging from 750 °C to 820 °C) to strain the ferrite and the coiling temperature high enough (above 600 °C) to recrystallize it.[6] Bearing in mind that the inner and outer layers, as well as the edges, cool faster than the center, the coiling temperature should generally be kept between 700 °C and 650 °C in an industrial line. In consequence, it is very difficult to obtain a fully recrystallized material after coiling in the thinnest sheets due to thermal losses.

Several authors proposed a new strategy,[7,8,9] which consists of transferring a hot coil (of 2- to 4-mm-thick sheet) from the hot strip mill directly to an additional rolling stand. After recoiling, a heavy warm deformation is performed below the γ-α transformation temperature to reduce the thickness down to 1.2 mm or less, followed by recoiling. For higher ferrite rolling temperatures, the final product may be obtained directly, but for lower ferrite rolling temperatures, an additional postannealing treatment will be necessary after coiling. The conditions of this last rolling process and the subsequent heat treatment are of vital importance to obtain fully recrystallized material.

The AlN precipitation during thermomechanical processing can play an important role in improving deep drawing properties by assisting the formation of specific texture components during recovery and recrystallization.[10–13] The goal of the present article is to study the influence of ferritic warm rolling parameters together with coiling conditions on the microstructural evolution of ELC steels.

II. MATERIAL AND EXPERIMENTAL PROCEDURE

The chemical composition of the ELC steel analyzed in this work is presented in Table I.

The coil transfer operation between the two partial processes, *i.e.*, hot strip mill and heavy warm deformation, is simulated by an isothermal hold for 15 minutes at intermediate coiling temperatures ranging from 580 °C to 700 °C. After isothermal holding, a heavy deformation reduction (hereafter defined as heavy warm reduction (HWR)) between 35 and 65 pct is given at temperatures ranging from 530 °C to 630 °C. Specimens are subsequently cooled at 4 °C/s to 5 °C/s to the desired coiling temperature. The processing parameters of specimens analyzed are presented in Table II. Rectangular samples 2 mm in width and 30 mm in length (parallel to the rolling direction) were machined from as-quenched material.

Recrystallization of the heavy warm-deformed material takes place during the subsequent coiling process. The industrial coiling process was simulated by an annealing cycle at a certain temperature (coiling temperature) for 1.5 hours. The simulated coiling temperatures ranged from 525 °C to 700 °C. Samples were heated at 50 °C/s to the annealing temperature, held for 1.5 hours at this temperature, and subsequently helium-jet quenched to room temperature.

The annealing cycles were performed using the heating and cooling devices of an Adamel Lhomargy LK02 high-resolution dilatometer described elsewhere.[14] The heating device consists of a very low thermal inertia radiation furnace in a gas-tight enclosure enabling testing under vacuum or an inert atmosphere. The power radiated by two tungsten filament lamps is focused on the specimen by means of a bielliptical reflector. The temperature is measured with a 0.1-mm-diameter chromel-alumel (type K) thermocouple welded to the specimen. Cooling is carried out by blowing a jet of helium gas directly onto the specimen surface. The helium flow rate during cooling is controlled by a proportional servovalve.

The samples were mounted in bakelite and subsequently ground and polished according to standardized techniques for metallographic examination. Subsequently, they were

C. CAPDEVILA and F.G. CABALLERO, Tenured Scientists, J.P. FERRER, Postdoctoral Student, and C. GARCIA DE ANDRÉS, Senior Researcher, Department of Physical Metallurgy, are with the Centro Nacional de Investigaciones Metalúrgicas (CENIM), Consejo Superior de Investigaciones Científicas (CSIC), 8040 Madrid, Spain. Contact e-mail: ccm@cenim.csic.es

Manuscript submitted May 5, 2005.

Table I. Chemical Composition in Weight Percent

C	Mn	P	Si	S	Al	N
0.03	0.17	0.009	0.005	0.006	0.041	0.003

Table II. Specimen Processing Parameters

Sample	CT* (°C)	Deformation T** (°C)	HWR (Pct)
ELC-C	640	590	46
ELC-F	680	631	66
ELC-H	690	634	48
ELC-I	660	608	55
ELC-L	580	536	54

*CT = coiling temperature.
**Temperature at which heavy warm deformation takes place.

etched with Nital–2 pct solution for 35 to 45 seconds to reveal the microstructure by optical microscopy, or with picral reagent (4 g picric acid in 100 mL ethanol) to disclose the presence of cementite.[15] Measurements of recrystallized volume fraction were performed statistically by a systematic manual point counting procedure.[16] A grid superimposed on recorded micrographs, covering the sectioned plane of the sample, provides an unbiased statistical estimation of recrystallized volume fraction after a suitable number of placements.

The evolution of the recovery-recrystallization processes or precipitation processes was studied by means of thermoelectric power (TEP) measurements. A schematic representation of the TEP apparatus is given elsewhere.[17] The experimental procedure of the TEP measurement is the following: the sample is pressed between two blocks of a reference metal (in this case, pure iron). One of the blocks is at 15 °C, while the other is at 25 °C to obtain a temperature difference ΔT. A potential difference ΔV is generated at the reference metal contacts. The apparatus does not give the absolute TEP value of the sample (S^*), but a relative TEP (ΔS) in comparison to the TEP of pure iron ($S_0{}^*$) at 20 °C. The value of ΔS is given by the following relation:

$$\Delta S = S^* - S_0{}^* = \frac{\Delta V}{\Delta T} \quad [1]$$

The TEP value does not depend on the shape of the sample, which is a great advantage of this technique. Moreover, the measurement is performed very quickly (less than 1 minute) and precisely (about ±0.5 pct). The resolution is of the order of 1 nV/K.

Since analysis of very-small-sized particles was required (AlN particles), it was decided to produce carbon extraction replicas. Extraction replicas make it possible to examine relatively large areas of a sample in the transmission electron microscope compared to thin foils. Carbon replicas were prepared according to the Fukami ''two-step replica method.''[18] Samples were polished in the usual way and then etched with Nital–2 pct reagent. A small amount of methyl acetate was dropped and spread on the surface of the specimen. Before volatilization of the solvent, a cellulose acetate film was laid over the specimen. After a few minutes, the film was peeled off from the specimen. Subsequently, to avoid curling of the material, it was kept for about 30 minutes in an oven heated at 80 °C. Then, the film was put into a high vacuum chamber for carbon deposition. Finally, the cellulose acetate layer was dissolved in a sequence of acetone baths. A copper mesh was used to support carbon replicas that were examined in a JEOL* JEM-200 CX transmission electron microscope operating at 200 keV.

*JEOL is a trademark of Japan Electron Optics Ltd., Tokyo.

The thermodynamic calculations involved here have been performed using the commercial software package developed by the National Physics Laboratory (NPL) and called MTDATA.[19] The evolution of carbon in solid solution into ferrite with temperature and cementite precipitation have been calculated with this software.

III. RESULTS AND DISCUSSION

The materials listed in Table II present a deformed microstructure. The higher the deformation, the more elongated is the grain structure. Figure 1 shows, as an example, the microstructure of samples with the lowest and the highest HWR: ELC-C and ELC-F, respectively.

A. *Cementite Particle Morphology before Annealing*

Etching with picral reagent revealed differences of cementite morphology in samples with different coiling temperatures (Figure 2) in the as-quenched state. It can be concluded from the figure that higher coiling temperatures (ELC-H, ELC-F, and ELC-I samples) induce finer cementite particles along grain boundaries together with isolated coarse particles. As the coiling temperature decreases (ELC-C and ELC-L samples), the fine cementite particles tend to disappear and the coarse ones are more numerous.

The microstructures of Figure 2 demonstrate that cementite morphology and distribution in the microstructure after heavy warm deformation are intimately related to coiling temperature, which is consistent with that previously reported in the literature.[20] According to MTDATA calculations, most of the cementite precipitation in the steel takes place in a temperature range between 727 °C and 577 °C (Figure 3). Therefore, at a coiling temperature of 580 °C, a large amount of coarse cementite precipitation occurs during the transfer process itself. In contrast, as the coiling temperature is increased, to temperatures around 660 °C, the amount of cementite formed during the transfer is smaller. Hence, the coarse cementite particles become more scarce. Moreover, due to the level of carbon in solid solution in ferrite at these temperatures (Figure 3), some additional coarsening takes place during the transfer. This leads to a precipitate network formed by fewer, coarser cementite particles as compared with steels with low transfer temperature (Figures 2(d) and (e)).

If the transfer temperature is high enough, most of the coarse cementite particles are avoided. Therefore, most of the carbon remains in solid solution and will precipitate during cooling and the subsequent heavy warm deformation

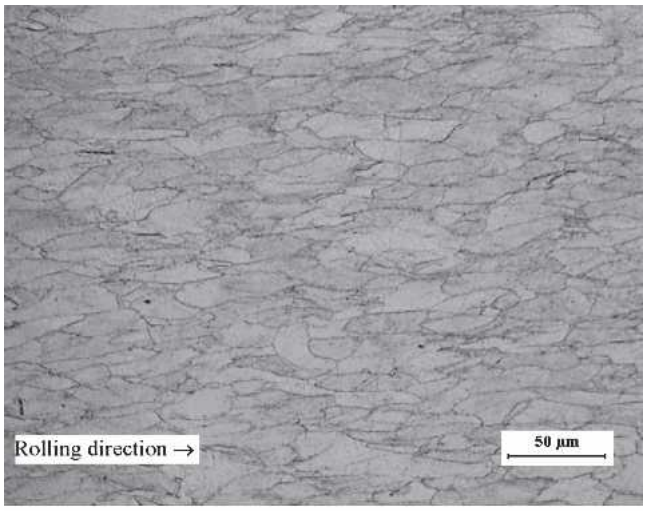

(*a*)

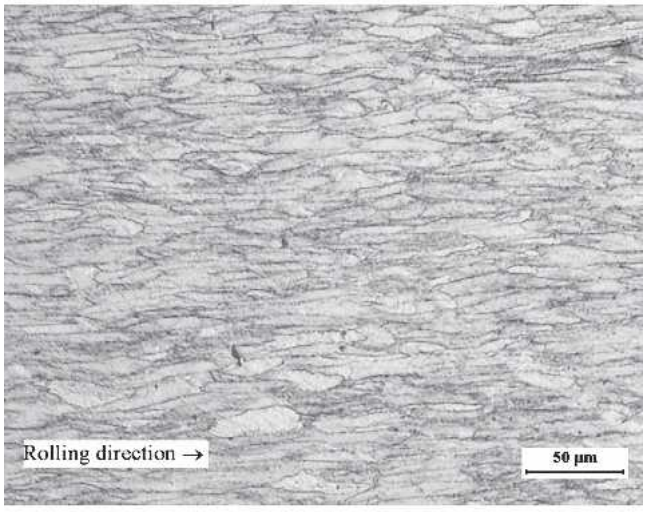

(*b*)

Fig. 1—As-received microstructure: (*a*) ELC-C and (*b*) ELC-F (Nital–2 pct etching).

process to form a network of small particles located at the grain boundaries. This is consistent with experimental results, which reveal that a large number of grain boundary cementite particles appear on steel with the highest deformation temperature (Figures 2(a) and (b)). Finally, it seems reasonable to consider that the entire carbon content has precipitated to form cementite after the heavy warm deformation process.

B. *Evolution of Second-Phase Particles during Annealing*

In this section, the effect of the annealing cycle on second-phase particles, simulating industrial coiling conditions after heavy warm deformation is described. Figure 4 shows the evolution of TEP measurements in the different samples for annealing temperatures ranging from 525 °C to 700 °C. A detailed analysis of the TEP results presented in this figure reveals two common patterns worth noting. First, higher TEP values are recorded in samples with high coiling temperature (ELC-F, ELC-H, and ELC-I) as compared with those with low coiling temperature (ELC-C and ELC-L). Second, the same TEP value is reached on annealing at 700 °C for all of the samples studied. In addition, a progressive drop in TEP is detected down to a minimum value reached at 625 °C to 650 °C, independent of the coiling temperature.

It is clear that at higher annealing temperatures, the amount of cementite particles is lower (Figure 5). Moreover, theoretical calculations of the evolution of carbon in solid solution predicted by MTDATA have been carried out (Figure 3). The variation of the TEP value due to a change of carbon concentration ([C]) can be expressed as follows:

$$\Delta S^{\text{rel}} = K_{\text{C}}[\text{C}] \qquad [2]$$

where ΔS^{rel} is the relative TEP value between the as-quenched sample after the heavy warm deformation process and the annealed sample, [C] is the carbon concentration in wt pct, and K_{C} is the TEP constant for carbon in solid solution for which a value of $-45\ \mu$V/K (wt pct) has been proposed.[21]

Figure 6 shows the expected evolution of ΔS^{rel} according to those calculations. It is clear that a good correlation between experimental and calculated results is observed on annealing below 600 °C. However, a clear discrepancy is observed for temperatures above 600 °C. While theoretical calculations predict a significant drop of the TEP, experimental results revealed that TEP increases for annealing temperatures above 600 °C. This rise in TEP, together with the aforementioned effect of coiling temperature, could be related to AlN precipitation.

The solubility product for the aluminum nitride reaction in terms of weight percent of the components (indicated by square brackets) is given by[12]

$$\log([\text{Al}][\text{N}]) = -(6770/T) + 1.033 \qquad [3]$$

where T is the absolute temperature. Figure 7(a) shows the relationship between dissolved aluminum and nitrogen at five different temperatures. For the steel studied that contained 0.003 wt pct N, it can be seen that total dissolution will occur at ~900 °C, provided that just the stoichometric amount of aluminum (~0.01 wt pct) is present. However, with an aluminum content of ~0.04 wt pct, as in the present steel, it is necessary to increase the temperature to ~1200 °C in order to ensure full decomposition of AlN. This is already achieved since the soaking temperature is 1200 °C, but precipitation of AlN must also be prevented during, and immediately after, hot rolling. Leslie *et al.*[22] studied the rate of precipitation and found a characteristic C-curve with a maximum rate at about 800 °C. Thus, to avoid AlN precipitation, it is necessary to cool rapidly between 900 °C and 600 °C. In practice, this is achieved by water-spray cooling after hot rolling, which gives a cooling rate similar to that employed to cool to the transfer temperature.

For this reason, ELC-C and ELC-L samples, where transfer was undergone at ~650 °C and ~600 °C, respectively, present the lowest TEP values. This is consistent with the assumption that most of the Al and N are still in solid solution in these materials. By contrast, steels ELC-F,

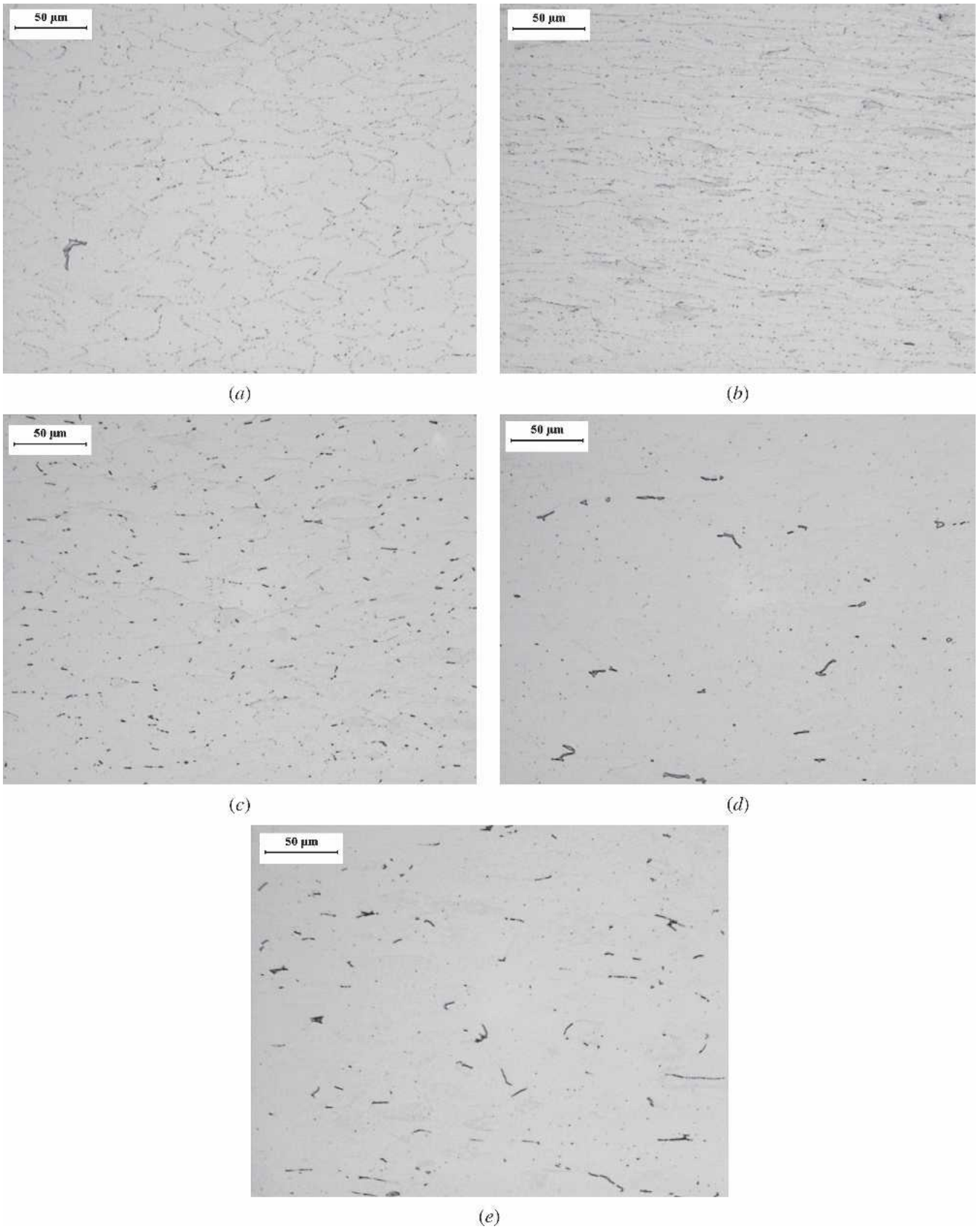

Fig. 2—Cementite distribution in the as-received material: (*a*) ELC-H, (*b*) ELC-F, (*c*) ELC-I, (*d*) ELC-C, and (*e*) ELC-L (Picral etching).

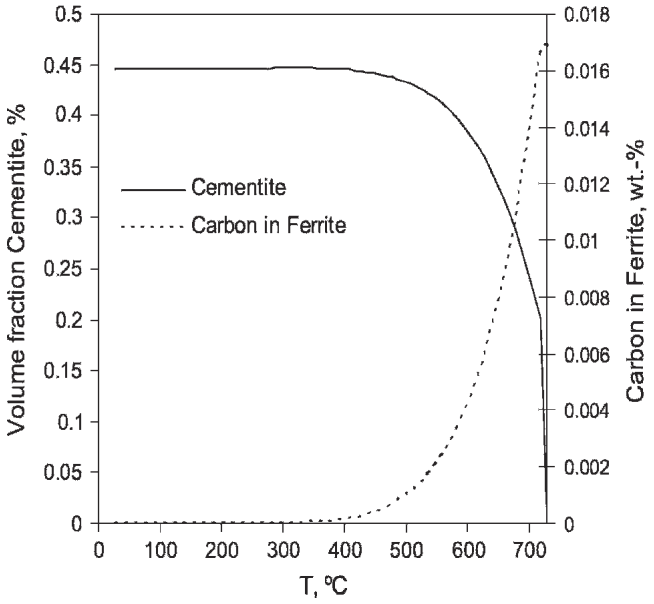

Fig. 3—Evolution of cementite and carbon in solid solution in ferrite (MT-DATA calculations) with annealing temperature.

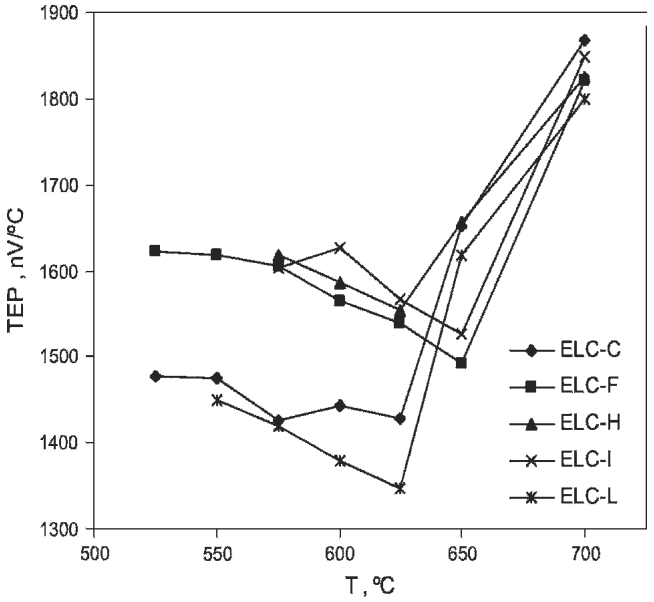

Fig. 4—TEP evolution with annealing temperature.

ELC-H, and ELC-I, where transfer was done at around 700 °C, present higher TEP values, which indicate that some AlN precipitation has occurred during transfer and the heavy warm deformation.

The rise in TEP at temperatures above 625 °C during the reheating cycles can also be explained on the basis of AlN precipitation. As was mentioned previously, AlN precipitation takes place at temperatures between 600 °C and 900 °C with a maximum around 800 °C. Thus, reheating above 600 °C will induce AlN precipitation leading to the subsequent TEP increase. Moreover, the similar results achieved in all the materials after annealing at 700 °C suggest that most of the AlN precipitation has taken place at these annealing temperatures, which is fully consistent with

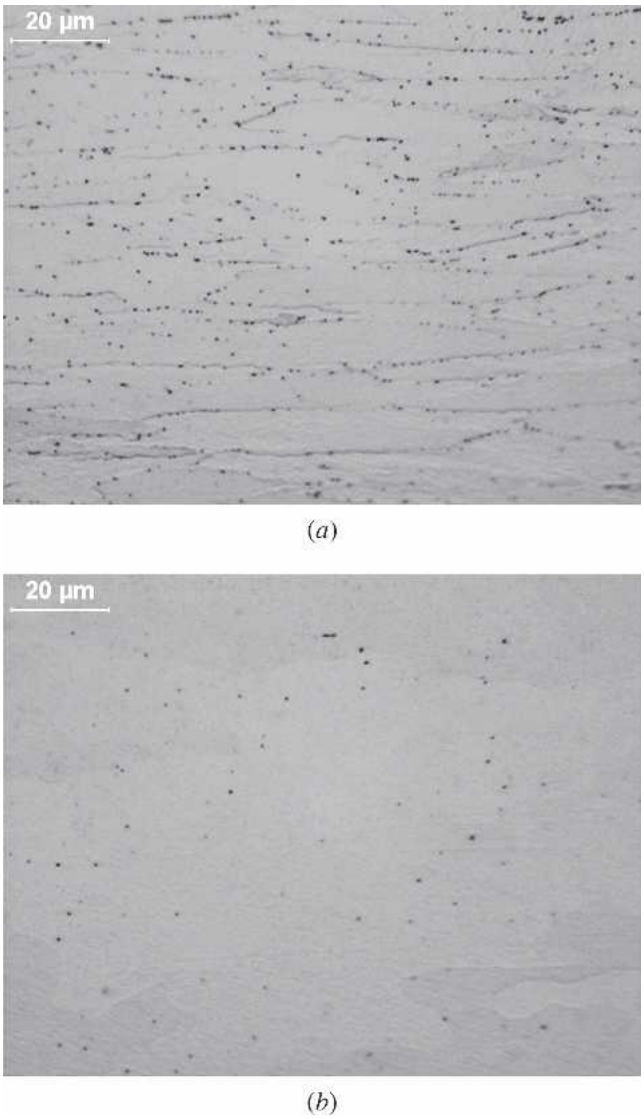

Fig. 5—Cementite morphology in ELC-F steel after annealing at (*a*) 575 °C and (*b*) 625 °C.

Figure 7(b), where the end of AlN precipitation is achieved at 700 °C after ~1.5 hours.

The presence of AlN precipitates was revealed by TEM examination of carbon extraction replicas of all the samples listed in Table II. While no identification of AlN precipitates was possible in the as-received material, these precipitates were successfully identified in samples heat treated at 700 °C (Figure 8). From this figure, it is clear that the precipitates are located along the subgrain boundaries prior to recrystallization. This result is consistent with other reported studies,[11,23] as will be analyzed in Section C.

C. *Influence of AlN Precipitation on Recrystallized Grain Morphology*

The recrystallization start temperature is defined as the temperature at which a volume fraction of 1 pct of recrystallized grains is found after 1.5 hours of annealing. Figure 9 shows the hardness and recrystallized volume fraction evolution with annealing temperature (after 1.5 hours

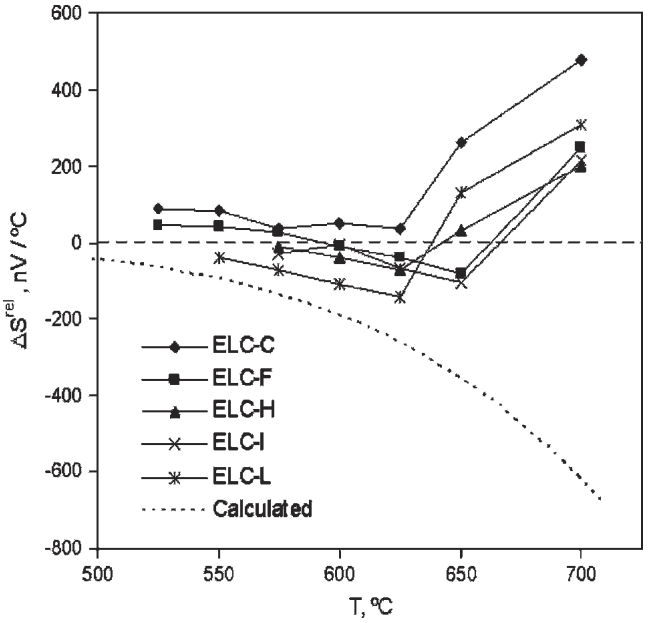

Fig. 6—Actual and predicted evolution of TEP with annealing temperature.

annealing). Comparison of both figures shows that an increase of the recrystallized volume fraction corresponds to a proportional decrease of the hardness.

A delay in the beginning of recrystallization is detected as the coiling temperature is increased in samples with the same degree of deformation. In this sense, the start of recrystallization in ELC-H samples is delayed with regard to ELC-C, and in ELC-I with regard to ELC-L. The samples with the lowest coiling temperature (ELC-C and ELC-L) and the highest HWR (ELC-F) present the lowest recrystallization start temperature (Figure 9(b)). It is also worth mentioning that the evolution of recrystallization seems to slow in ELC-C and ELC-L at temperatures between 600 °C and 625 °C, *i.e.,* recrystallization is retarded. Such behavior is accompanied by a plateau in the hardness curve (Figure 9(a)). This phenomenon is also observed in ELC-I but at slightly higher temperatures (between 625 °C and 650 °C).

Figure 10 shows the evolution of the mean recrystallized grain size and the number of recrystallized grains per unit volume (n) with annealing temperature. Two different tendencies can be distinguished: samples ELC-C, ELC-F, and ELC-L present a smaller grain size and higher values of n as annealing temperature is increased up to 650 °C; on the other hand, ELC-H and ELC-I present increasing grain size and hence decreasing n values as annealing temperature is increased. The highest grain size is recorded at 650 °C in ELC-H, and at 700 °C in ELC-I.

Summarizing the results presented in Figure 9 and 10, two different behaviors can be distinguished: samples where the onset of recrystallization occurs at low temperatures, *i.e.*, ELC-C, ELC-F, and ELC-L, present smaller grain sizes and higher values of n, which indicates that recrystallization occurs rapidly in these materials. By contrast, those samples with higher recrystallization start temperatures, ELC-H and ELC-I, present longer grain sizes and smaller n values, which seems to indicate that the progress of recrystallization is more difficult in these samples.

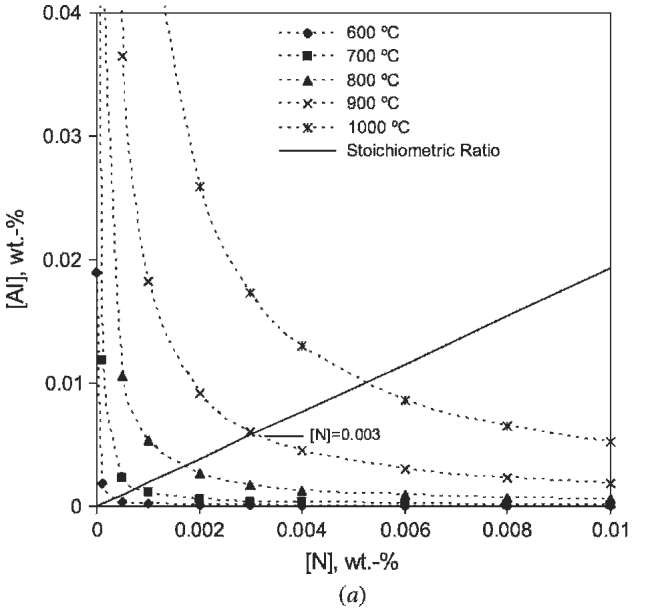

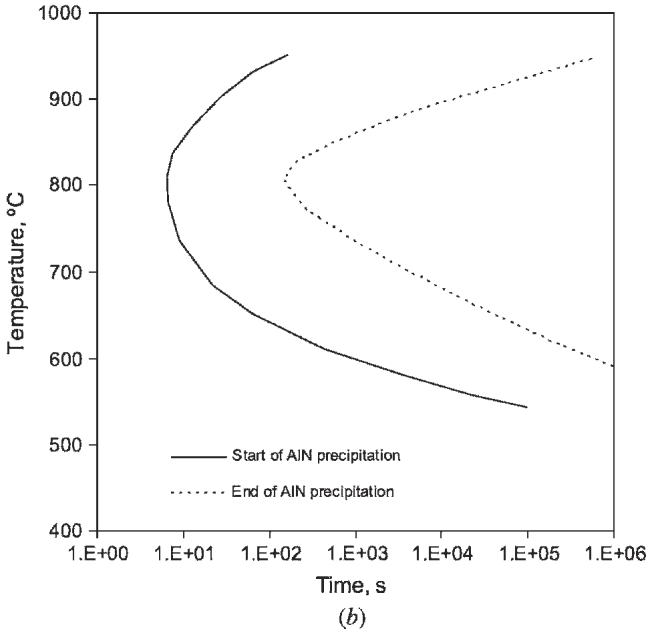

Fig. 7—(*a*) Plot of solubility product of AlN in austenite at various temperatures and (*b*) TTT diagram for AlN precipitation in steel.[22]

It has been extensively reported that second-phase particles strongly influence the shape and size of recrystallized grains.[24] Likewise, while coarse particles may accelerate recrystallization,[25,26] fine ones may retard or even completely inhibit such process.[25,27] The transition between both behaviors is mainly a function of the volume fraction of second-phase, F_v, and the particle radius, r. When the F_v/r ratio is less than 0.2 μm^{-1}, recrystallization is accelerated by providing preferential nucleation sites.[27,28] In this sense, coarse cementite particles are often preferential nucleation sites in low-carbon steels.[29] On the other hand, several authors claim that the formation of fine clusters of Al and N impairs the growth of subgrains and, therefore,

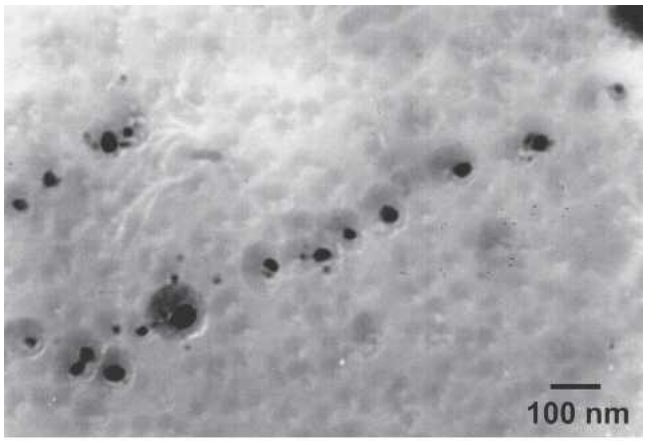

(*a*)

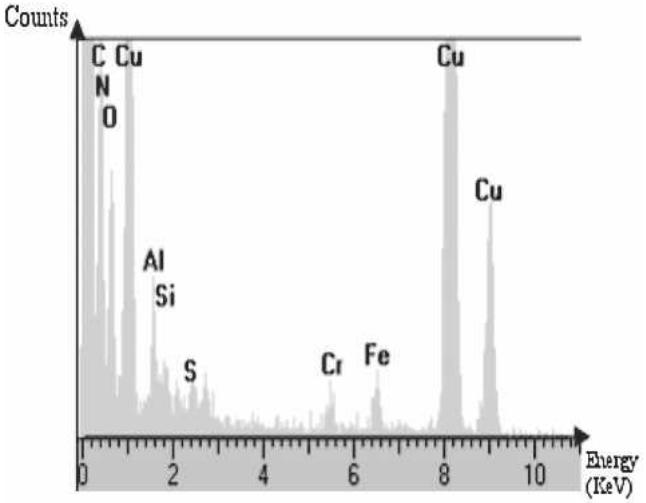

(*b*)

Fig. 8—(*a*) Alignment of AlN precipitates and (*b*) EDS spectrum.

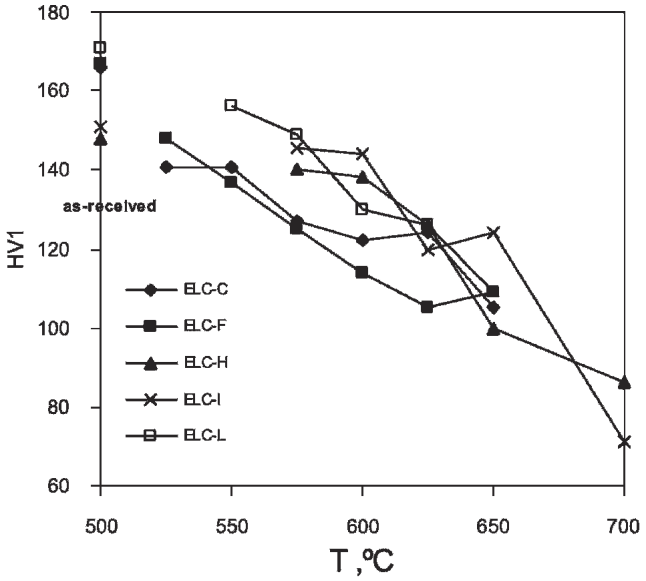

(*a*)

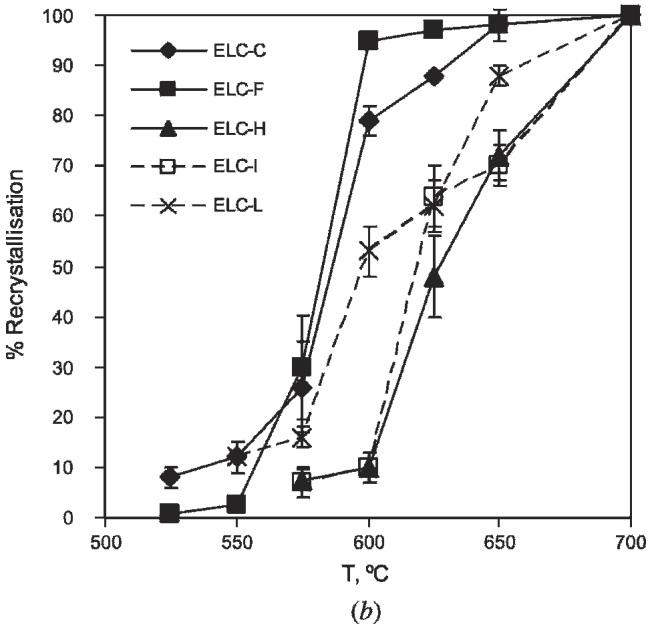

(*b*)

Fig. 9—Evolution of (*a*) hardness and (*b*) recrystallization volume with annealing temperature (1.5 h holding time).

the nucleation of recrystallized grains.[10,30] These clusters appear mainly on subgrain boundaries, which generally develop parallel to the rolling direction. The low nucleation density together with the fine dispersion of AlN particles then promotes formation of an irregular and coarse recrystallized grain with anisotropic growth.

Aubrun[31] studied such precipitation-recrystallization interactions after cold rolling in low-carbon steels, and established two different annealing temperature ranges that lead to an equiaxed or an irregular grain microstructure after recrystallization. In agreement with these studies, if the temperature and heating rate are high enough to promote recrystallization before precipitation, there is no influence of precipitates, and the resulting recrystallized grain microstructure will be equiaxed. However, if the annealing temperature or heating rate is low enough, precipitation will take place during recovery and recrystallization, promoting a coarse and irregular grain microstructure after recrystallization. Moreover, the precipitation of small particles such as AlN may lead to the arrest of recrystallization. Longer times or higher temperatures are needed to promote the coarsening of precipitates so that the recrystallization process may finish. This phenomenon was called ''double recrystallization'' or ''recrystallization into the transition zone'' by Aubrun,[30] and leads to the coarsest and most anisotropic grain.

According to this, the behavior observed in the warm-rolled samples is consistent with AlN precipitation and the morphology of cementite particles in the as-rolled material. Thus, Figure 4 shows the lowest TEP values for ELC-C and ELC-L, which indicate that most of the Al and N is in solid solution. Therefore, no AlN particles are present at the beginning of recrystallization, and the start of recrystallization is not delayed. Likewise, the existence of coarse cementite particles promotes recrystallization. The nucleation near large nondeformable cementite particles is

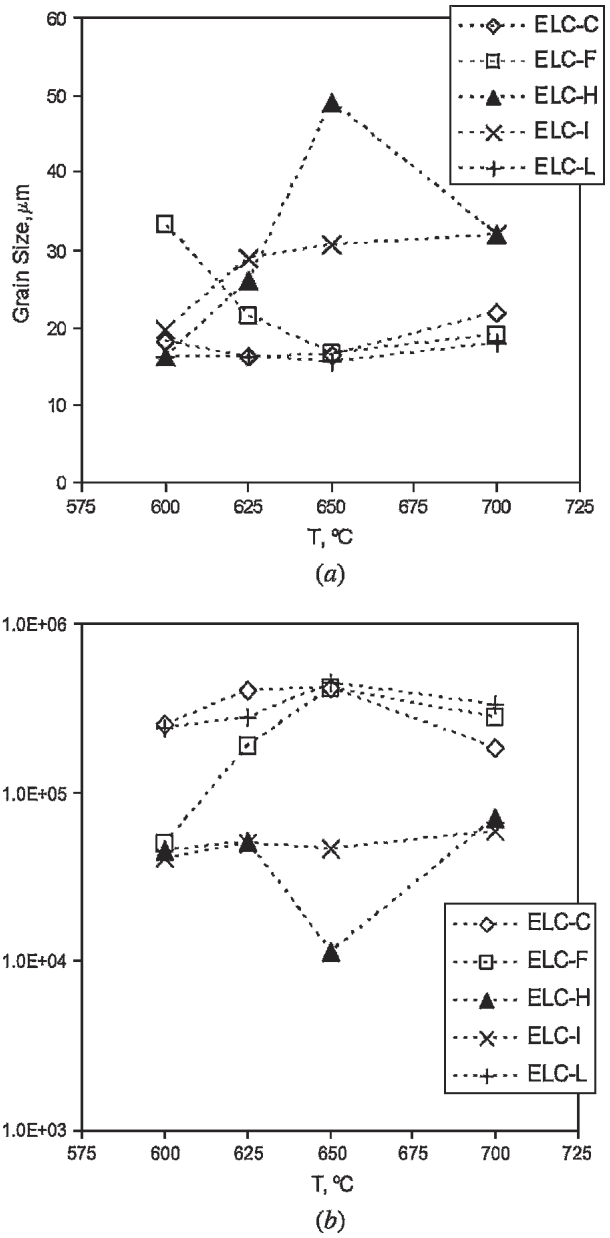

Fig. 10—Evolution of (*a*) grain size and (*b*) number of recrystallized grains per unit volume with annealing temperature.

described in the literature.[32,33,34] It is concluded that recrystallized grains nucleated in deformation zones around coarse particles, and this nucleation is more prominent at lower temperatures. Hence, the lowest recrystallization start temperature and smallest grain size are recorded.

By contrast, ELC-H and ELC-I present relatively fine cementite particles that are not a favorable condition for nucleation. Likewise, higher TEP values for these samples (Figure 4) reveal the existence of AlN particles. It is generally accepted that recrystallization, and in particular, nucleation, is greatly retarded by AlN precipitation,[22,23,35–37] leading to higher recrystallization start temperature and coarser grain sizes.

Attention should be paid to the ELC-F material. Because of the high HWR, the driving force for recrystallization is so intense that recrystallization proceeds easily even though some AlN particles are present and cementite particles are very fine.

On the other hand, the recrystallized grain morphology depends on the annealing temperature. Thus, grains tend to be coarser and more anisotropic for lower annealing temperatures. This effect is more pronounced in steels deformed at higher temperatures, *i.e.*, ELC-F, ELC-H, and ELC-I. This is illustrated in Figures 11(a) and (b), where the microstructures obtained after annealing ELC-F samples at 600 °C and 625 °C are presented. It is clear from the figures that a higher annealing temperature leads to more isotropic grains. The reduced nucleation frequency and the extended growth range of the new grains formed at low annealing temperatures, combined with the tendency for AlN precipitation to occur in ''sheets'' on prior grain boundaries and sub-boundaries extended in the rolling plane, induce the formation of a characteristic ''pancake'' microstructure. As the reheating temperature increases, more coalescence of AlN particles occurs. This, together with the increasing driving force for recrystallization, tends to increase the number of recrystallized grains. Consequently, finer and more isotropic grains are obtained (Figures 10 and 11(a) and (b)).

In contrast, the ELC-H steel, *i.e.*, the material with the lowest degree of deformation and the highest deformation temperature, presents a different behavior, as illustrated in Figures 11(c) and (d). In this case, a higher annealing temperature induces coarser and more irregular recrystallized grains. This could also be related to the plateau in the evolution of recrystallization found from 600 °C to 650 °C (Figure 9). The onset of AlN precipitation is consistent with the rise in TEP values noted in Figure 4. This precipitation could inhibit the growth of new recrystallized grains, leading to the plateau in Figure 9. These results are consistent with theories for abnormal subgrain growth by Humphreys.[38,39] These suggest that, assuming AlN precipitates preferentially on subgrain boundaries, Zener pinning of these boundaries will allow low-angle boundaries to migrate but prevent high-angle boundaries from doing so. Boundaries that break away from these pinning particles will experience a lower pinning value and hence an accelerated growth. This induces the formation of coarse grains.

Samples with low deformation temperature or with higher HWR (ELC-C, ELC-L, and ELC-F) recrystallize before 600 °C, and hence no precipitation-recrystallization interaction will take place. Only when recrystallization is shifted to temperatures above 600 °C (ELC-L) can arrest be observed. On the other hand, in samples with high deformation temperature or with low HWR (ELC-H and ELC-I), the small driving force for recrystallization leads to significant retardation of this: recrystallization then occurs simultaneously with AlN precipitation, promoting the formation of irregular and coarser grains (Figures 9 and 11(b)). This fact is especially evident for ELC-H samples. However, if the reheating temperature is high enough, recrystallization finishes before precipitation of AlN takes place. This explains why ELC-H grain sizes are smaller and more regular in shape after 1.5 hours at 700 °C as compared to the grains at low annealing temperature.

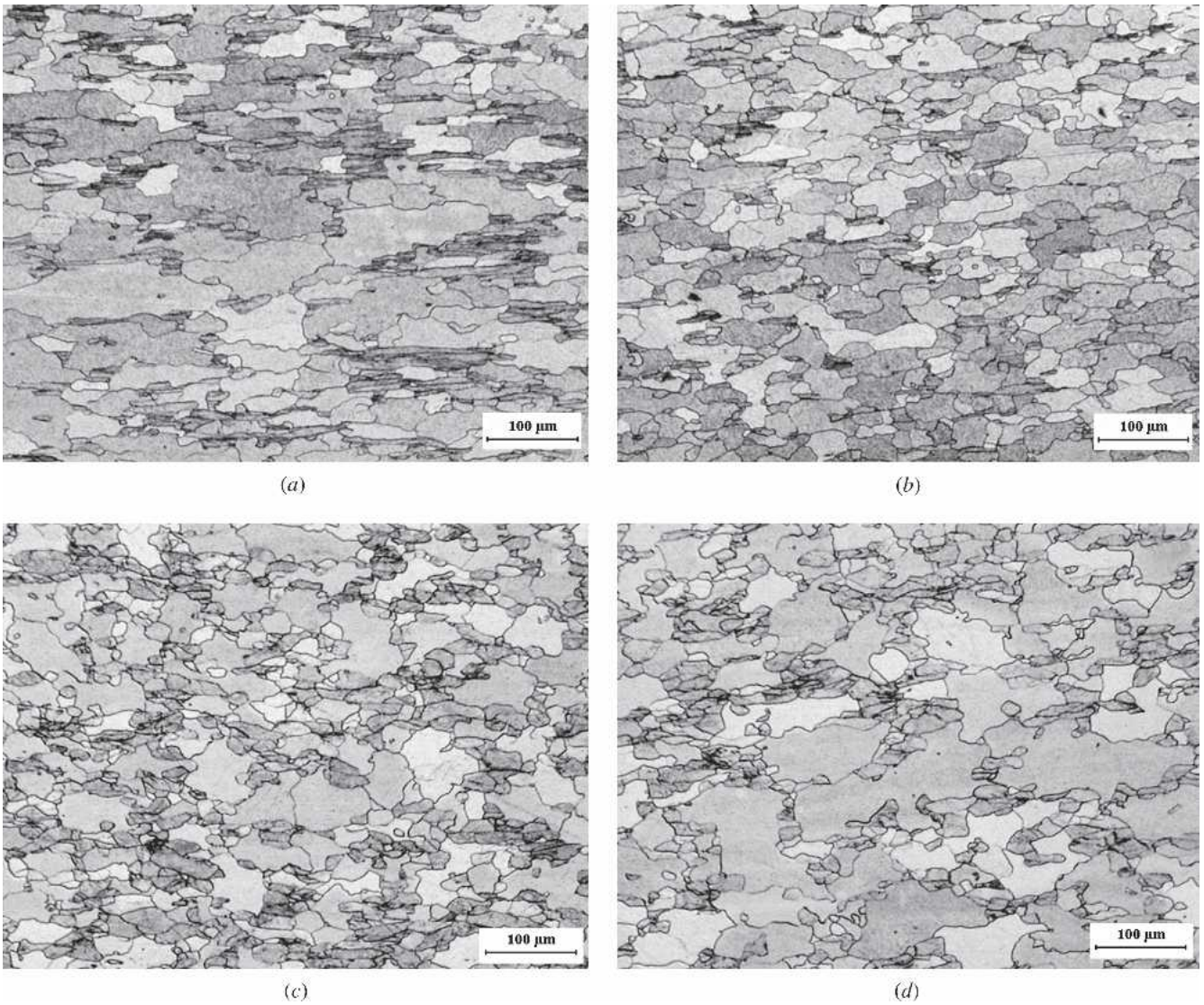

Fig. 11—Annealed ELC-F microstructure after (*a*) 600 °C, 1.5 h; and (*b*) 625 °C, 1.5 h. ELC-H after (*c*) 625 °C, 1.5 h; and (*d*) 650 °C, 1.5 h (2 pct Nital etching).

IV. CONCLUSIONS

1. The recrystallization process in heavy warm-rolled ELC steel has been studied. The results obtained after different warm-rolling conditions and reheating temperatures have been analyzed to conclude that a slight modification of the heavy warm deformation conditions induces considerable differences in subsequent recrystallization during reheating.
2. The transfer temperature between the hot-rolling mill and the heavy warm deformation mill produces two kinds of cementite particles: coarser particles formed during the transfer itself, decreasing in size and increasing in number as the transfer temperature decreased, and fine particles precipitated on grain boundaries during the heavy warm deformation process itself.
3. The absence of AlN precipitation, together with the existence of coarse cementite particles and a higher stored energy, produces finer and more equiaxed recrystallized grains in materials with high HWR or low coiling temperatures.
4. A high transfer temperature promotes AlN precipitation during transfer. This precipitation, together with the low stored energy for recrystallization because of low HWR, leads to coarser and irregularly shaped recrystallized grains after subsequent reheating. A low transfer temperature leads to a small amount of AlN precipitation during transfer.
5. The low stored energy in samples with high coiling temperatures and low HWR induce the overlapping of recrystallization and AlN precipitation, leading to the inhibition of recrystallization.

ACKNOWLEDGMENTS

The authors acknowledge financial support from the European Coal and Steel Community (Grant No. ECSC-7210-PR-351) and from the Spanish Ministerio de Educación y Ciencia (MEC) (Grant No. MAT2002-10811-E). One of the authors (JPF) expresses his gratitude to MEC for the financial support in the form of a Ph.D. grant (FPI

Program). The authors thank Professor D.G. Morris for his useful comments and his time editing the manuscript.

REFERENCES

1. D. Liu, A.O. Humphreys, M.R. Toroghinezhad, and J.J. Jonas: *Iron Steel Inst. Jpn. Int.,* 2002, vol. 42, pp. 751-59.
2. M.R. Barnett and J.J. Jonas: *Iron Steel Inst. Jpn. Int.,* 1991, vol. 39, pp. 856-73.
3. M.R. Barnett, J.J. Jonas, and P.D. Hodson: *37th Mechanical Working and Steel Processing Conf.,* I. Sadler, ed., ISS, Warrendale, PA, 1996, vol. XXXIII, pp. 971-77.
4. A.O. Humphreys, D.S. Liu, M.R. Toroghinezhad, and J.J. Jonas: *Iron Steel Inst. Jpn. Int.,* 2002, vol. 42 (Suppl.), pp. S52-S56.
5. M.R. Toroghinejad, A.O. Humphreys, F. Ashrafizadeh, A. Najafizadeh, and J.J. Jonas: *Mater. Sci. Forum,* 2003, vols. 426–432, pp. 3691-96.
6. A. De Paepe and J.C. Herman: *41st MWSP Conf. Proc.,* I. Sadler, ed., ISS, Warrendale, PA, 1999, vol. XXVII, p. 951.
7. J.C. Herman, A. De Paepe, and V. Leroy: *Thermec '97,* Int. Conf. on Thermomechanical Processing of Steels and Other Materials, T. Chandra and T. Sakai, eds., TMS, Warrendale, PA, 1997, pp. 507-14.
8. ECSC-Project No. 710-PA-PC/036 (97-D3.04a-c), Draft Final Report, Mar. 2001.
9. E. Vasseur, H. Réglé, E. Pinto Da Costa, and Y. Raulet: *Proc. Int. Conf. on Thermomechanical Processing of Steels,* May 24–26, 2000, IOM Communications, 2000, pp. 615-24.
10. Y. Meyzaud and P. Parnière: *Mém. Scientif. Rev. Métall.,* 1974, vol. LXXI, pp. 423-34.
11. J.T. Michalak and R.D. Schoone: *Trans. TMS-AIME,* 1968, vol. 242, pp. 1149-60.
12. W.B. Hutchinson: *Int. Met. Rev.,* 1984, vol. 29, pp. 25-42.
13. N. Lavaire, V. Massardier, and J. Merlin: *Scripta Mater.,* 2004, vol. 50, pp. 131-35.
14. C. García de Andrés, G. Caruana, and L.F. Alvarez: *Mater. Sci. Eng., A,* 1998, vol. A241, pp. 211-18.
15. F.S. Lepera: *J. Met.,* 1980, vol. 32, pp. 38-39.
16. G.F. Vander Voort: *Metallography. Principles and Practice,* McGraw-Hill Book Company, New York, NY, 1984, p. 427.
17. A. Ney and J. Luiggi: *Metall. Mater. Trans. A,* 1998, vol. 29A, pp. 2669-73.
18. A. Fukami: *Specimen Preparation Techniques for Electron Microscopy,* Jeol News, Tokio, 1967, pp. 5-7.
19. *Metallurgical and Thermochemical Databank,* National Physical Laboratory, Teddington, Middlesex, United Kingdom, 1996, p. 1.
20. R.K. Ray, J.J. Jonas, and R.E. Hook: *Int. Mater. Rev.,* 1994, vol. 39, pp. 129-57.
21. N. Lavaire, J. Merlin, and V. Sardoy: *Scripta Mater.,* 2001, vol. 44, pp. 553-60.
22. W.C. Leslie, R.L. Rickett, C.L. Dotson, and C.S. Watson: *Trans. ASM,* 1954, vol. 46, pp. 1470-99.
23. R.H. Goodenow: *ASM Trans. Q.,* 1966, vol. 59, p. 804.
24. N. Hansen: *Mém. Scientif. Rev. Métall.,* 1975, vol. 72, pp. 189-203.
25. F.J. Humphreys: *Acta Metall.,* 1977, vol. 25, pp. 1321-44.
26. U. Koster: *Recrystallization of Metallic Materials,* F. Haessner, ed., Dr. Riedler Verlag, Stuttgart, 1971, p. 215.
27. F.J. Humphreys and M. Hatherly: *Recrystallization and Related Annealing Phenomena,* Pergamon Press, Oxford, United Kingdom, 1995, p. 127.
28. F.J. Humphreys: *Met. Sci.,* 1979, vol. 13, pp. 136-45.
29. H. Inagaki: *Iron Steel Inst. Jpn. Int.,* 1994, vol. 34 (4), pp. 313-21.
30. Ph. Aubrun and P. Rocquet: *Mém. Scientif. Rev. Métallurg.,* 1973, vol. LXX (4), pp. 260-69.
31. Ph. Aubrun and P. Rocquet: *Mém. Scientif. Rev. Métallurg.,* 1973, vol. LXX (7–8), pp. 569-75.
32. H. Inagaki: *Z. Metallkd.,* 1987, vol. 78, pp. 630-38.
33. H. Inagaki: *Z. Metallkd.,* 1993, vol. 82, pp. 99-107.
34. H. Inagaki: *Z. Metallkd.,* 1993, vol. 82, pp. 26-33.
35. A. Brahmi and R. Borrelly: *Acta Mater.,* 1997, vol. 45, pp. 1889-97.
36. V. Massardier, V. Guétaz, J. Merlin, and M. Soler: *Mater. Sci. Eng. A,* 2003, vol. A355, pp. 299-310.
37. V. Massardier, V. Guétaz, J. Merlin, and M. Soler: *Mater. Sci. Forum,* 2003, vols. 426–432, pp. 1267-72.
38. F.J. Humphreys: *Acta Mater.,* 1997, vol. 45, pp. 4231-40.
39. F.J. Humphreys: *Acta Mater.,* 1997, vol. 45, pp. 5031-39.